



## Unraveling ancient hexaploidy through multiply-aligned angiosperm gene maps

Haibao Tang, Xiyin Wang, John E. Bowers, et al.

*Genome Res.* 2008 18: 1944-1954 originally published online October 2, 2008

Access the most recent version at doi:[10.1101/gr.080978.108](https://doi.org/10.1101/gr.080978.108)

---

**References** This article cites 51 articles, 20 of which can be accessed free at:  
<http://genome.cshlp.org/content/18/12/1944.full.html#ref-list-1>

### License

**Email Alerting Service** Receive free email alerts when new articles cite this article - sign up in the box at the top right corner of the article or [click here](#).



---

To subscribe to *Genome Research* go to:  
<https://genome.cshlp.org/subscriptions>

---

Copyright © 2008, Cold Spring Harbor Laboratory Press

## Methods

# Unraveling ancient hexaploidy through multiply-aligned angiosperm gene maps

Haibao Tang,<sup>1,2</sup> Xiyin Wang,<sup>1,3</sup> John E. Bowers,<sup>1</sup> Ray Ming,<sup>4</sup> Maqsudul Alam,<sup>5</sup> and Andrew H. Paterson<sup>1,2,6</sup>

<sup>1</sup>Plant Genome Mapping Laboratory, University of Georgia, Athens, Georgia 30602, USA; <sup>2</sup>Department of Plant Biology, University of Georgia, Athens, Georgia 30602, USA; <sup>3</sup>College of Science, Hebei Polytechnic University, Tangshan, Hebei 063000, China; <sup>4</sup>Department of Plant Biology, University of Illinois at Urbana–Champaign, Champaign, Illinois 61801, USA; <sup>5</sup>Advanced Studies in Genomics, Proteomics and Bioinformatics, University of Hawaii, Honolulu, Hawaii 96822, USA

Large-scale (segmental or whole) genome duplication has been recurring in angiosperm evolution. Subsequent gene loss and rearrangements further affect gene copy numbers and fractionate ancestral gene linkages across multiple chromosomes. The fragmented “multiple-to-multiple” correspondences resulting from this distinguishing feature of angiosperm evolution complicates comparative genomic studies. Using a robust computational framework that combines information from multiple orthologous and duplicated regions to construct local syntenic networks, we show that a shared ancient hexaploidy event (or perhaps two roughly concurrent genome fusions) can be inferred based on the sequences from several divergent plant genomes. This “paleo-hexaploidy” clearly preceded the rosid–asterid split, but it remains equivocal whether it also affected monocots. The model resulting from our multi-alignments lays the foundation for approximating the number and arrangement of genes in the last universal common ancestor of angiosperms. Comparative analysis of inferred homologous genes derived from this model shows patterns of preferential gene retention or loss after polyploidy and reveals large variability of nucleotide substitution rates among plant nuclear genomes.

[Supplemental material is available online at [www.genome.org](http://www.genome.org).]

Ancient genome duplications are evident for many lineages of fungi (Kellis et al. 2004), animals (Jaillon et al. 2004), and plants (Bowers et al. 2003), offering opportunities for the evolution of new (Spillane et al. 2007) or modified (Hittinger and Carroll 2007) gene functions, altering gene dosages, and creating new gene arrangements. Traces from past whole-genome duplication events can often be detected from pairwise syntenic segments, including two sets of retained paralogs that have maintained relative genomic locations on syntenic chromosomes. In angiosperms, genome duplications are recurring in many lineages (Bowers et al. 2003), generating large numbers of paralogous loci.

Gene loss at duplicated loci effectively fractionates ancestral linkage patterns and reduces the density of continuous stretches of “paleologous” gene pairs, which are the remaining signatures of paleo-polyploidy (Thomas et al. 2006). Depending on the level of gene loss, the remaining signatures of duplication are sometimes so eroded that the homologous segments can no longer be identified based only on similarity to one another. The problem is multiplied when the species in question has undergone several genome duplications, with recent duplications tending to obscure synteny from more ancient events as is found in most angiosperm genomes. Such highly degenerate duplicated segments have been referred to as “ghost duplications” and can often be resolved by comparison to an appropriate “outgroup” genome

that did not experience polyploidy or undergo massive gene loss (Van de Peer 2004). For example, “bridging” of ghost duplications using outgroups has clarified the history of polyploidy in both *Saccharomyces* and *Tetraodon* (Jaillon et al. 2004; Kellis et al. 2004; Scannell et al. 2007).

Continuous stretches of duplicate genes can be computationally deduced through synteny, using some variants of clustering approaches (Vandepoele et al. 2002; Hampson et al. 2005) or more specifically using dynamic programming with a customized scoring scheme if conserved gene order (collinearity) is also considered (Haas et al. 2004; Wang et al. 2006). Traditional methods for deduction of synteny based on “best-in-genome” criteria (Miller et al. 2007), uncovering one-to-one best matching regions during pairwise genome comparisons, are relatively straightforward in vertebrates yet difficult in angiosperms because of additional challenges that are more prominent in angiosperm genomes (Tang et al. 2008). These challenges include frequent genome duplications and convoluted genome shuffling (rearrangements, chromosomal fusions and fissions), such as the extensive rearrangement that has occurred in *Arabidopsis* within the past 5 million years (Kuittinen et al. 2004).

One approach for the computational de-convolution of paleopolyploidy for deduction of ancestral gene orders is a bottom-up approach in which one attempts to resolve one duplication event at a time, starting with the most recent one. This is exemplified by studies in *Arabidopsis* and *Paramecium* where the most recently duplicated segments are merged to generate hypothetical intermediate profiles that are further recursively merged (Bowers et al. 2003; Aury et al. 2006).

Herein, we elaborate on an alternative top-down approach

## Corresponding author.

E-mail [paterson@uga.edu](mailto:paterson@uga.edu); fax (706) 583-0160.

Article published online before print. Article and publication date are at <http://www.genome.org/cgi/doi/10.1101/gr.080978.108>.

**Table 1.** Summary of sequenced plant genomes based on respective genome publications

Species	Assembly status <sup>a</sup>	Assembled/estimate size	Annotation version	Annotated gene no.
<i>Arabidopsis</i> ( <i>Arabidopsis thaliana</i> )	BAC-by-BAC	115 Mb/160 Mb	TAIR version 7	26784
Papaya ( <i>Carica papaya</i> )	WGS, N50 = 11 kb	278 Mb/372 Mb	University of Hawaii	25536
Poplar ( <i>Populus trichocarpa</i> )	WGS, N50 = 125 kb	410 Mb/485 Mb	JGI version 1.1	45554
Grape ( <i>Vitis vinifera</i> )	WGS, N50 = 65 kb	468 Mb/487 Mb	Genoscope release	30434
Rice ( <i>Oryza sativa</i> ssp. <i>japonica</i> )	BAC-by-BAC	371 Mb/389 Mb	RAP release 2 <sup>b</sup>	29389

<sup>a</sup>(BAC) Bacterial artificial chromosome; (WGS) whole-genome shotgun; (N50) maximum length  $L$  such that 50% of all bases are in contigs of length at least  $L$ .

<sup>b</sup>We only used mapped representative loci for the rice annotation project (RAP) release (Itoh et al. 2007).

(Tang et al. 2008) that is conceptually more attractive in that it only requires one cycle of deduction—first searching for pairwise synteny information and then combining the resulting pairs to form a multi-way correspondence among all structurally similar chromosomal segments. The efficacy of the top-down approach, however, depends on the searching strategy because of the degenerate synteny resulting from post-duplication gene loss. In particular, a top-down search strategy can incorporate “ghost duplications” (Van de Peer 2004), which are not discernible using a bottom-up approach based on information from only one species.

New angiosperm genome sequences (Table 1) promise to qualitatively improve our deductions about the evolution of angiosperm gene repertoire and arrangement. *Arabidopsis* (*Arabidopsis* Genome Initiative 2000), rice (*Oryza sativa*) (International Rice Genome Sequencing Project 2005), poplar (*Populus trichocarpa*) (Tuskan et al. 2006), grapevine (*Vitis vinifera*) (Jaillon et al. 2007), and papaya (*Carica papaya*) (Ming et al. 2008) have been sequenced, and more are in the pipeline. Indeed, *Arabidopsis thaliana*—a leading botanical model—is now known to be a relatively difficult system from which to deduce ancient gene orders. For example, many *Carica* segments show collinearity with three or four *Arabidopsis* segments, showing that two genome duplications have affected the *Arabidopsis* lineage since its divergence from *Carica* (Ming et al. 2008). Individual *Arabidopsis* genome segments correspond to only one *Carica* segment, showing that *Carica* has not duplicated since its divergence from *Arabidopsis*. Both *Vitis* and *Carica* have only one duplication event,  $\gamma$ , while  $\alpha$  and  $\beta$  occurred in the *Arabidopsis* lineage after its divergence from the *Carica* lineage (Ming et al. 2008; Tang et al. 2008).

Some newly sequenced genomes have less complicated genome structure and thus may represent better models for comparative genomics than *Arabidopsis*. In this study, we exploit fragmentary conservation of plant gene orders from multiple genomes along with a new top-down algorithm MCscan, to improve deductions about the course of angiosperm genome structural evolution.

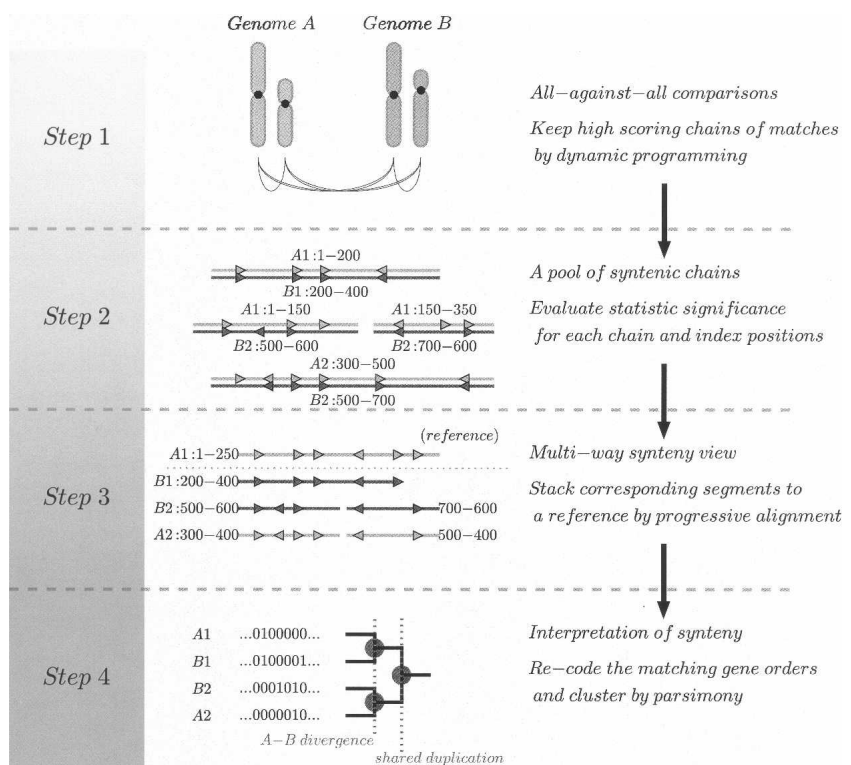
## Results

### MCscan: Algorithm for multiple gene order alignments

When several genomes and subgenomes (resulting from ancient duplication events) are compared simultaneously, synteny and collinearity between all possible pairs of genomes are tedious to enumerate because chromosomal homology is “transitive.” For example, if there are corresponding chromosomal regions in three genomes A, B, and C, comparisons between the genomes would reveal three pairwise synteny blocks (A-B, B-C, A-C), whereas it could be better represented as a single multiple synteny block (A-B-C). To solve this problem, we implemented a novel algorithm, MCscan, that exploits this transitivity property of collinearity to perform multiple alignments by incorporating pairwise synteny that is derived from shared evolutionary events.

The algorithm involves a four-stage pipeline illustrated in Figure 1, with each individual stage described in further detail in Methods.

We first use a sequence similarity search program to detect

**Figure 1.** Flow-chart of MCscan core algorithm.

matchings among genes in all possible pairs of chromosomes and scaffolds and in both transcriptional directions. This is followed by the “pairwise collinearity” stage, in which the neighboring matches are chained along using dynamic programming. The pairwise collinear blocks are combined in the “multi-collinearity” stage, by fixing one gene order as reference and then heuristically stacking the pairwise synteny tracks one after another. In this step, we need to use a “reference” gene order as the basis for stacking the tracks; we then describe the aligned synteny blocks as “threaded by the reference order,” a procedure inspired by TBA aligner (Blanchette et al. 2004). Once the multi-syntenic blocks are identified, we can classify the segments and index them to different evolutionary events, mainly duplications and divergence.

As a result, MCscan condenses the combinatorial matches between multiple chromosomal segments resulting from divergence and recursive duplication events and creates a view of the multiply-aligned segments.

### Patterns of synteny conservation

Using the top-down algorithm MCscan, we have aligned large portions of the five sequenced genomes (*Arabidopsis*, *Carica*, *Populus*, *Vitis*, and *Oryza*) based on synteny. A total of 61% of the *Arabidopsis* genes have preserved their ancestral locations based on cross-species synteny (Table 2), versus 44%, 51%, and 46% of *Carica*, *Populus*, and *Vitis* genes, respectively.

The variation in frequencies of aligned genes might be due to different levels of synteny conservation in different species. However, it is also correlated with the degree of contiguity of the respective sequences (Table 1), with a higher percentage of genes explained by synteny in the genomes with higher N50. Indeed, if most genes are in small or unanchored scaffolds, it would be very difficult for MCscan to detect them as syntenic, even if they do remain in their ancestral locations.

Alignments with gene order preserved across four eudicot species show clear triplicated structure in many local regions. Each triplicated branch contains orthologous segments from up to four *Arabidopsis* regions, one *Carica* region, two *Populus* regions, and one *Vitis* region, supporting the hypothesis that this genome triplication ( $\gamma$ ) occurred in a common ancestor of all four species; *Populus* has one duplication event ( $p$ ) in its salicoid lineage, and *Arabidopsis* has two duplications ( $\alpha$  and  $\beta$ ) in its crucifer lineage. The multiple alignments were threaded by *Vitis* as the reference order (Supplemental Data 1), since *Vitis* appeared to have the most close-to-ancestral karyotype among the genomes that we investigated (Jaillon et al. 2007). This is likely to

change in the future when we include additional genomes; however, using *Vitis* as the current “reference” would produce the best solution so far.

The triplication of gene loci is also evident from Table 2. For example, we found that 88 aligned loci in *Carica* have multiplicity levels of three (triplication  $\gamma$ ), with only one aligned locus exceeding a multiplicity of 3; 54 aligned loci in *Populus* have the expected multiplicity level of 6 (triplication  $\gamma \times$  duplication  $p$ ), but only three loci exceed 6. The loci that exceed the expected multiplicity level are likely produced by additional small-scale (single gene or segmental) duplications in each lineage.

### Further circumscribing the $\gamma$ duplication event

The  $\gamma$  duplication event was previously dated to have occurred after the monocot–dicot separation but before the expansion of the rosids (Jaillon et al. 2007). We investigated the lower boundary of this claim by sampling genomic regions from other eudicots outside the rosids for which long, contiguous sequences (BACs) were available in GenBank, including tomato (*Solanum lycopersicum*) and banana (*Musa acuminata*).

We first mapped unigenes onto 194 sequenced tomato (*Solanum lycopersicum*) BACs as preliminary gene annotation and inspected synteny to *Vitis*. Among the 78 *Solanum* BACs that have more than 10 distinctively mapped unigenes, 72 have more than 50% of genes showing primary synteny to a single *Vitis* chromosome (Supplemental Data 2). Each individual tomato BAC corresponds closely to only one of the triplicate regions rather than showing equal matches to each of the three  $\gamma$  paleo-homeologous chromosomes in *Vitis*. Figure 2A shows one example of a *Solanum* BAC that aligns to the *Vitis* gene order. Although the *Solanum* BACs that we inspected only represent ~2.5% of the genome, the evidence so far strongly supports the hypothesis that  $\gamma$  triplication occurred in a common ancestor of asterids and rosids. Under this scenario, each *Solanum* segment would be expected to have up to four primary syntenic segments in *Arabidopsis*, as has been suggested (Ku et al. 2000).

Based on a similar notion, Jaillon et al. (2007) calculated the relative abundance of one-to-three cases between *Oryza* and *Vitis* and suggested that the triplication occurred after the monocot–dicot split. It is tempting to push the dating of  $\gamma$  further, yet we consider such dating to have uncertainties in view of current evidence. Contrary to the well-conserved synteny within the eudicot group, only 14% of *Oryza* genes could be placed in cross-species gene clusters (Table 2). This proportion represents the actual extent of collinearity between *Oryza* and any of the four eudicots, as *Oryza* is the only monocot genome included in this

**Table 2.** Number of clustered groups of genes at different multiplicity levels in five angiosperm species

Species	Multiplicity level										No. of ancestral loci	No. of genes (%)	WGD or segmental expansion
	1	2	3	4	5	6	7	8	9	10			
<i>Arabidopsis</i>	6742	2642	868	282	80	32	6	5	1	1	10,659	16,451 (61%)	54%
<i>Carica</i>	9118	942	88 <sup>a</sup>	1	0	0	0	0	0	0	10,149	11,270 (44%)	11%
<i>Populus</i>	5147	6362	763	618	96	54 <sup>a</sup>	3	0	0	0	13,043	23,457 (51%)	80%
<i>Vitis</i>	9926	1671	239 <sup>a</sup>	15	2	0	0	0	0	0	11,853	14,055 (46%)	18%
<i>Oryza</i>	2197	685	140	35	9	2	0	0	0	0	3068	4184 (14%)	36%

The statistics are based only on groups that contain genes from at least two different species, as constructed from syntenic alignments. The number of inferred ancestral loci is calculated by  $\sum_{m=1}^{10} N_m$ , and the number of genes that maintain their ancestral positions is calculated by  $\sum_{m=1}^{10} m \cdot N_m$ , where  $m$  is the multiplicity level varying from 1 to 10 and  $N_m$  is the number of groups for each multiplicity level.

<sup>a</sup>Expected multiplicities for *Carica*, *Populus*, and *Vitis*. The multiplicity for *Arabidopsis* is 12 (yet no gene groups retained all 12 copies), and equivocal for *Oryza*.

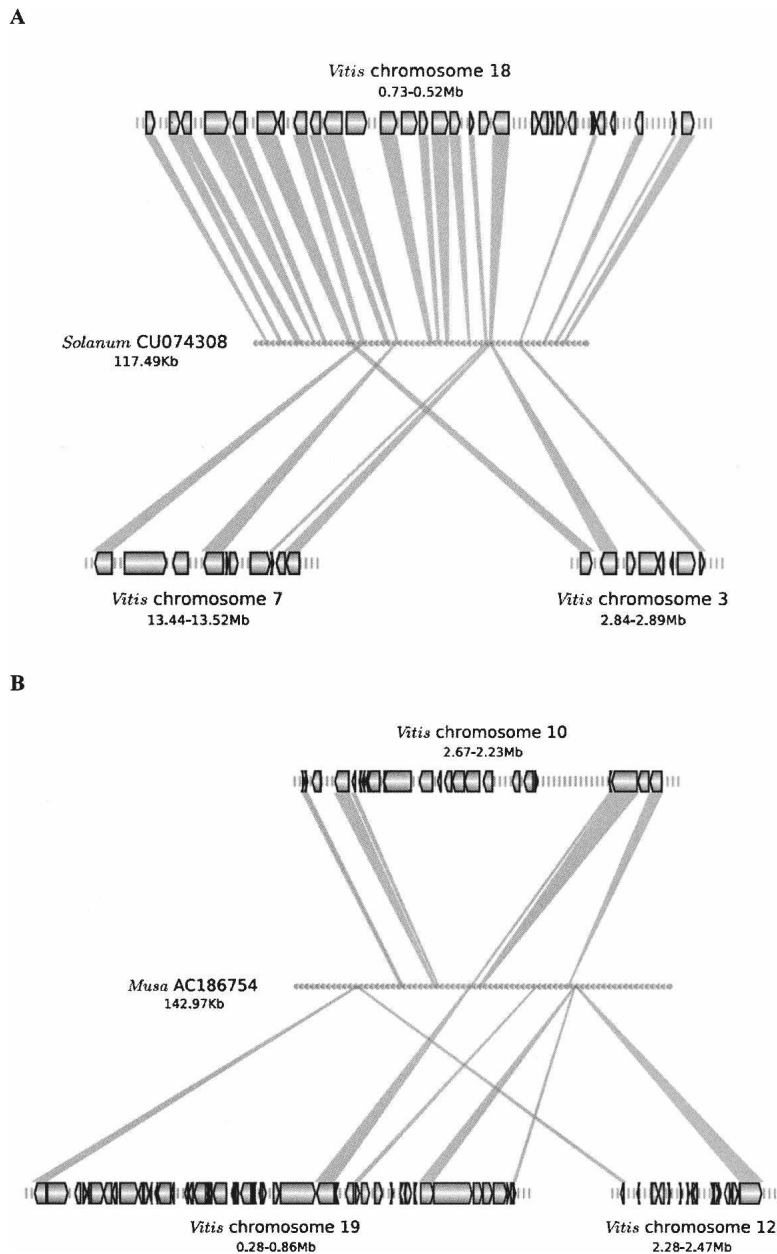


**Figure 2.** Collinearity between triplicate *Vitis*  $\gamma$ -homeologous regions with BAC sequences from *Solanum* (A) and *Musa* (B). (Black glyphs) Genes with the tip showing the transcriptional direction; (gray shades) syntenic matches between a *Vitis* gene and *Solanum* or *Musa* sequences.

study. Therefore, it is more difficult to make accurate inference of synteny patterns because of the greater evolutionary distance involved and additional duplication in the cereal lineage. While several studies hinted that additional monocot duplication(s) predated the cereal duplication  $\rho$  (Zhang et al. 2005; Jaillon et al. 2007), whether such additional duplication(s) found in *Oryza* correspond to the  $\gamma$  triplication we saw in core eudicots remains to be determined.

We also examined synteny to *Vitis* for chromosomal regions from a monocot species that is basal to the cereals—banana (*Musa acuminata*). On average, the levels of synteny between *Musa* BACs and *Vitis* chromosomes are 50% lower than synteny between *Solanum* and *Vitis*. Furthermore, in contrast to the one-

to-one primary synteny pattern of *Solanum* and *Vitis*, *Musa* BACs show roughly equal matches to any of the three  $\gamma$  homeologs in *Vitis* (Fig. 2B), a pattern similar to *Oryza-Vitis*. However, failure to detect one-to-one (as opposed to one-to-three) correspondence between monocot regions and *Vitis* cannot be viewed as strong evidence that  $\gamma$  occurred after the eudicot–monocot split. An alternative but equally plausible scenario is that the monocots and eudicots share  $\gamma$  but diverged soon after  $\gamma$  occurred. Under this scenario, the gene arrangements between two orthologous chromosomes would share very little synteny because of stochastic, independent gene losses in both lineages—leading to similarly low levels of correspondence of chromosome in one taxon to each of its three  $\gamma$  paralogs in another taxon.

While highly specific one-to-one synteny is indicative that two lineages share the  $\gamma$  triplication, frequent one-to-three synteny is not necessarily indicative that one lineage lacks the triplication. So far we can only confidently place the  $\gamma$  triplication before the asterid–rosid split and consider the status of the paleo-hexaploidy in the monocot lineage to be unclear.

It is difficult to test the hypothesis that the  $\gamma$  triplication predated the divergence of monocots and eudicots. For example, additional data from an outgroup genome such as *Amborella* would help, but does not necessarily solve the placement of the triplication if  $\gamma$  is found absent in that outgroup. Much of the uncertainty is rooted in the fact that the  $\gamma$  triplication is an ancient event that at least predated the asterids–rosids, and comparisons across this evolutionary distance are often less effective. Therefore, we need broader and more judicious sampling of plant taxa. Indeed, fortuitous discoveries of genomes like grapevine that have close-to-ancestral

karyotypes facilitate comparisons across major angiosperm clades. Similarly, additional karyotypically conserved monocot or basal angiosperm genomes that are free of recent polyploidies might better elucidate the scenario.

#### Comparisons of $\gamma$ paleologs show that triplicate subgenomes are mostly homogeneous

We tested whether any two of the three subgenomes are genetically closer to one another than the third. We retrieved  $\gamma$  paleolog groups that have retained genes from all three  $\gamma$  subgenomes, on different chromosomes or scaffolds in *Carica* or *Vitis*, the two genomes that are unaffected by additional duplications other

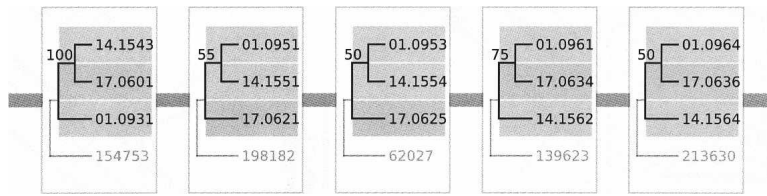


**Figure 3.** Topologies for five proximal  $\gamma$  ancestral loci that contain three collinear *Vitis* genes. *Vitis* gene names are abbreviated as “[chromosome],[gene index]” for graphing. Each tree was rooted using one best-matching moss gene, identified by JGI protein accession number. The numbers above branches are bootstrap values in the phylogenetic reconstruction. There are a total of 10 local blocks that have more than five triplets in *Carica* and *Vitis* that are studied in the same way. Phylogenetic analysis was performed using PHYLIP version 3.67 (Retief 2000). The analysis was carried out using the protdist program (default parameters) followed by neighbor-joining using neighbor. We used the seqboot program to simulate 100 bootstrap replicates and the consense program to retrieve one consensus tree.

than  $\gamma$ . We then inferred gene trees for these triplet groups under the assumption that if two subgenomes are, indeed, more similar to each other than to the third, we expect to see only one prevalent tree topology along paleolog groups within the same ancestral duplicated (triplicated) segment. Only a limited data set is suitable for this study since we need to have enough triplets along the three subgenomes that are derived from the same ancestral segment. We picked 10 blocks with five or more *Vitis* triplets (this cutoff was chosen arbitrarily as we need enough triplets within each block for inference, yet we do not have many blocks that have more than six or seven triplets). Nonetheless, we failed to find one dominant topology for any block, with a typical example shown in Figure 3. The fact that the  $\gamma$  subgenomes are indistinguishable from each other makes it unlikely that one of the triplicated subgenomes may have originated from large-scale segmental duplications or aneuploidy. Instead, the  $\gamma$  triplication may have been an ancient auto-hexaploidy formed from fusions of three identical genomes, or allo-hexaploidy formed from fusions of three somewhat diverged genomes. We are not able to determine whether the fusion(s) were a single event or two events a relatively short time apart (the latter case, e.g., characterizing the well-studied evolution of hexaploid wheat). A more definitive test of allo-hexaploidy versus auto-hexaploidy would only be possible if extant diploid parental species can be found, and this is unlikely since the genome duplications appear to be pervasive throughout most angiosperm clades including the basal lineages (Cui et al. 2006).

## Discussion

By exploiting fragmentary conservation of plant gene orders, together with a new top-down multi-alignment approach, limitations of *Arabidopsis* for comparative genomics are mitigated by using new angiosperm genome sequences to qualitatively improve our deductions about the tempo and modes of evolution of angiosperm genes and genomes.

### Rate variations between paleologs within four eudicot species

Deduction of a consensus gene order for multiple taxa permits us to directly compare estimates of the ages of gene duplications based on rates of nucleotide substitution per synonymous site ( $K_s$ ) between paleolog pairs (syntenic paralogs), filtering out the inevitable influence of background (i.e., single gene) duplications, which superimpose an L-shaped curve on the relics of whole-genome duplications (Blanc and Wolfe 2004; Cui et al.

2006). By excluding the single gene duplications, we were able to analyze the  $K_s$  distribution using mixtures of log-normals (see Methods).

Although  $\gamma$  apparently occurred in a common ancestor of *Carica*, *Populus*, and *Vitis*, the median  $K_s$  between *Vitis*  $\gamma$  paleologs (1.22) is much lower than that of *Carica* (1.76) and *Populus* (1.54) (Table 3). The median values of  $K_s$  among  $\gamma$  duplicates in these three genomes show highly significant difference (Kruskal-Wallis one-way ANOVA,  $P = 2.25 \times 10^{-142}$ ).

The  $K_s$  distributions analyzed with mixture models show the expected

number of components for each species, except for *Arabidopsis*, where we can find only two instead of three distinct components (Table 3). This two-peak distribution (Fig. 4B) is similar to the results of a previous study (Maere et al. 2005) even though MCscan provides better deductions about the identities of paleologs. We postulate that more rapid substitutions occur at synonymous sites in *Arabidopsis* than in the other three eudicot species, with *Arabidopsis*  $\gamma$  paleologs being saturated with synonymous substitutions. Therefore, within *Arabidopsis*,  $K_s$ -based distances between paralogs cannot differentiate  $\gamma$  duplicates from either the tail of the distribution of  $\beta$  duplicates, or from noise, or both. The median  $K_s$  values between *Arabidopsis*  $\beta$  and  $\gamma$  duplicates are close to saturation (2.00), much larger than those of the  $\gamma$  duplicates in the other three species (Table 3). Repeating the analysis using a more conservative genetic distance—transversion rate at fourfold degenerate sites (4DTV) (Fig. 4C) shows almost the same pattern as using  $K_s$ , suggesting that the saturation effect of DNA substitutions may have also affected 4DTV distance.

Differences in the median values of distances between the paralogs that are derived from the common  $\gamma$  event can be explained by different substitution rates among the four rosid lineages. We constructed a phylogenetic tree with per-branch  $K_s$  estimates, based on orthologous gene groups that are strictly single copy in all five species (Fig. 4D). The same trend was found, with increasing evolutionary rates in branches leading to *Vitis*, *Populus*, *Carica*, and *Arabidopsis*, respectively, suggesting that the variations of substitution rates are not confined to populations of duplicate genes but are rather lineage-specific. A similar range of nuclear rate variation in flowering plants has been documented in previous studies, and is often associated with life history (Gaut et al. 1996; Koch et al. 2000). In general, the short generation time in the annual *Arabidopsis* might have contributed to the fast substitution rates compared with *Populus* or *Vitis*,

**Table 3.** Mixture model estimates for distributions of  $K_s$  between paleologs in each species

Species	Sample size	No. of mixture components	Median	Variance	Proportion
<i>Arabidopsis</i>	7435	2	0.86	0.08	0.51
			2.00	0.20	0.49
<i>Carica</i>	907	1	1.76	0.32	1
<i>Populus</i>	13,113	2	0.27	0.01	0.62
			1.54	0.24	0.38
<i>Vitis</i>	2288	1	1.22	0.16	1

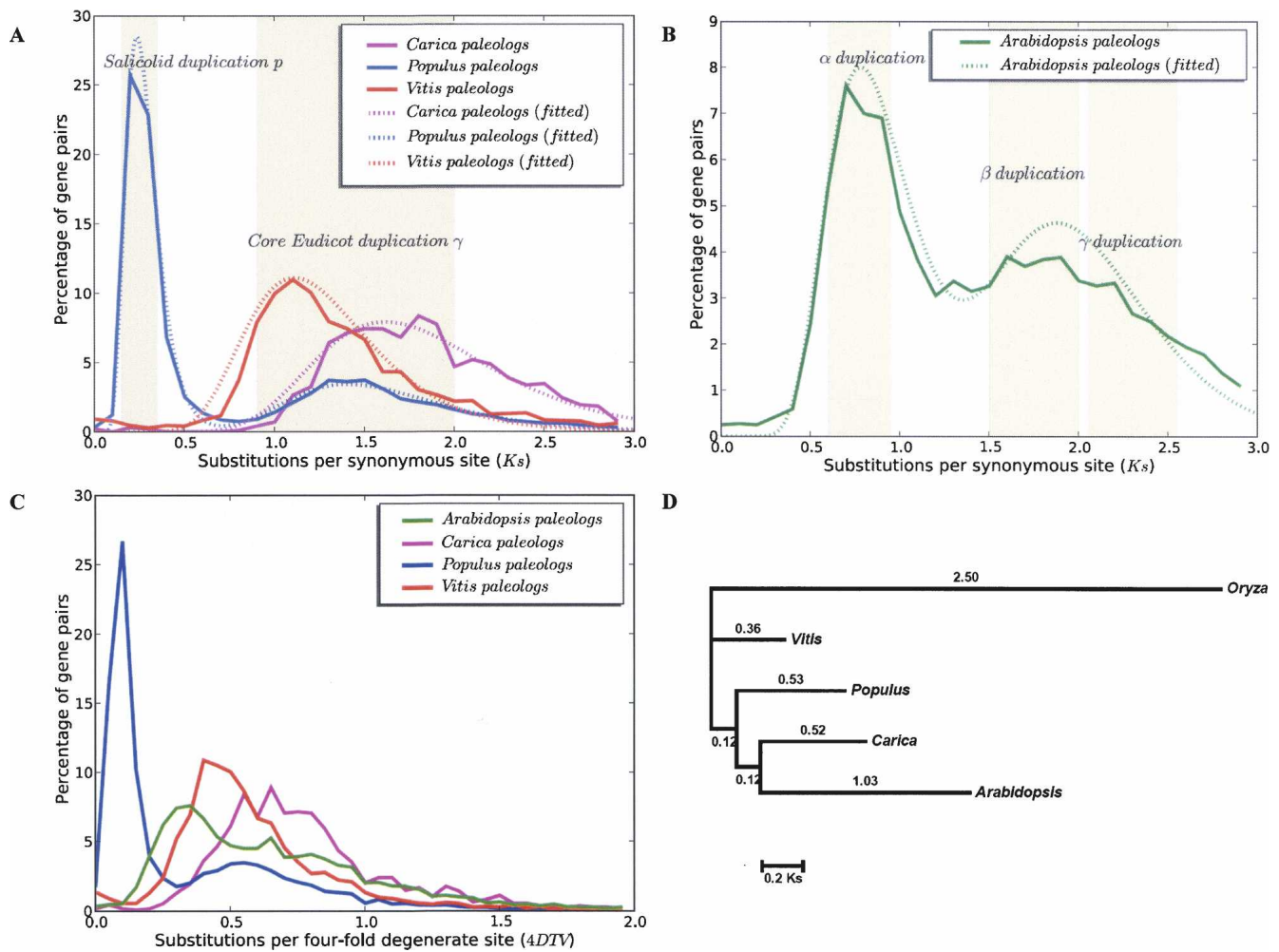


**Figure 4.** (A,B) Distribution of  $K_s$  distances among *Carica*, *Populus*, *Vitis*, and *Arabidopsis* paleologs.  $K_s$  values are grouped into bins of 0.1 intervals. Certain  $K_s$  intervals are highlighted as they correspond to several presumed whole-genome duplication events. Dotted lines are fitted mixtures of log-normal distributions for the paleolog  $K_s$  distributions (see Methods). (C) Distribution of 4DTV distance among paleologs in the same four eudicot lineages. (D) Phylogeny of single-copy ortholog set used in relative rate estimates. A total of 47 orthologous genes that are single copy in all five species were used in the analysis. Protein alignments for each ortholog group were constructed and then used to guide DNA alignments. The alignments are then concatenated, with 53,856 aligned nucleotide positions. Per-site  $K_s$  values on each branch were estimated by codeml in the PAML package (Yang 1997) using a constrained topology that reflects organismal relationships.

which are perennials. However, because life history attributes tend to change over evolutionary time, the generation-time effect is not sufficient to explain the rate heterogeneity among different organisms (Gaut et al. 1996).

Because substitution rates vary among lineages, timing of duplication or speciation events is hard to determine using genetic distance measures alone. For the same reason, dating of ancient events based on phylogenetic trees (Bowers et al. 2003; Tuskan et al. 2006) could produce incongruous results since the drastic differences in rates may lead to incorrect trees that are artifacts because of long-branch attractions (Felsenstein 2004).

One phylogenetic model placed *Vitis* within the eurosid I clade (Jaillon et al. 2007), in contrast with the prevailing view of the Vitaceae as sister to both eurosid I and eurosid II (Davies et al. 2004; Soltis et al. 2005). Indeed, *Populus* and *Vitis* do show small  $K_a$  or  $K_s$  values for substitutions between inferred orthologs (Table 4). However, the seemingly smaller distance between *Populus* and *Vitis* genes should be interpreted with caution since both species appear to have relatively slow evolutionary rates.

The striking differences in evolutionary rates among these taxa at the DNA sequence level may, in part, explain the controversial placement of *Vitis* inside the eurosids by some investigators (Jaillon et al. 2007). Indeed, we found that if we use *Arabidopsis* as the reference point, the increasing  $K_s$  distances from *Carica*, *Populus*, and *Vitis* appear to support the view that *Vitis* is an outgroup to the rosids (Table 4).

#### Inferring the number and arrangement of genes in the ancestral angiosperm

Top-down multiple alignments mitigate the fragmentation and decay of ancestral gene orders, improving our ability to deduce the number and arrangement of genes in the last common ancestor of a group of genomes. When we align gene orders to produce multiple collinear segments, corresponding genes are collected and merged into a deduced "ancestral locus." A total of 18,447 deduced ancestral loci (corresponding gene groups) collectively represent 77,059 genes in the five species we studied (see

**Table 4.**  $K_s$  and  $K_a$  values for syntenic orthologs of five sequenced plant genomes

	<i>Arabidopsis</i>	<i>Carica</i>	<i>Populus</i>	<i>Vitis</i>	<i>Oryza</i>
<i>Arabidopsis</i>	—	0.24	0.23	0.25	0.37
<i>Carica</i>	1.57 (6913)	—	0.17	0.19	0.35
<i>Populus</i>	1.64 (8366)	1.08 (8504)	—	0.16	0.31
<i>Vitis</i>	1.72 (7381)	1.12 (7920)	0.98 (10,143)	—	0.32

For each syntenic group, the smallest  $K_s$  or  $K_a$  value among all orthologous pairs was retrieved to represent the value. The lower triangle shows median  $K_s$  values, and the upper triangle shows median  $K_a$  values. Numbers in brackets correspond to the number of syntenic groups used in each comparison.  $K_s$  values between *Oryza* and four eudicots show saturated substitutions and high variances and therefore should not be considered reliable estimates.

Supplemental Data 3 for complete compilation). Among these loci, 3680 (20%) are specific to only one species, and 14,767 (80%) contain genes from at least two different species. We studied the compositions of the cross-species groups (Table 2). If all duplicates derived from each genome duplication event had been retained, each clustered ancestral locus ideally would have three *Carica* genes ( $\gamma$  only), three *Vitis* genes ( $\gamma$  only), six *Populus* genes ( $\gamma$ ,  $p$ ), and 12 *Arabidopsis* genes ( $\gamma$ ,  $\beta$ ,  $\alpha$ ). Such extreme cases were not observed. However, we still find cases in which the copy numbers are close to saturation in these genomes (Table 2), and two specific cases are further discussed in the next section.

Conceptually, the number of cross-species syntenic gene clusters would reflect the gene number prior to  $\gamma$ , by far the most ancient duplication detected by our collinearity algorithm. If we assume that most genes retain their ancestral positions, then by using only the set of genes that show cross-species synteny and correcting for the “inflation” induced by genome duplications, we can have a relatively accurate estimate of ancestral gene number. The four fully sequenced eudicots each yield slightly different estimates of this number, varying from 10,149 for *Carica* to 13,043 for *Populus* (Table 2). This range coincides closely with previous estimate of ancestral angiosperm gene numbers of 12,000–14,000 based an independent gene birth model (Sterck et al. 2007). Our number, however, may be an underestimate considering that the alignment algorithm does not achieve perfect sensitivity. Moreover, lower contiguity and less progress in annotation may tend to reduce the *Carica* number, and appreciable heterozygosity in the sequenced genotype (resulting in alleles sometimes being considered different loci) may somewhat inflate the *Populus* number.

In contrast to estimation of ancestral gene number, inference of ancestral gene order is a much harder problem, and our computationally reconstructed gene order should not be considered as truly “ancestral.” In our analysis, the inferred ancestral gene order was deduced by taking the consensus of the aligned gene orders among various chromosomes and scaffolds in the five species we investigated, similar to some previous approaches (Blanc et al. 2003). Ideally such consensus orders would be required to reflect all the gene arrangements aligned in the same block. However, the solution is not unique as there may be several possible consensus arrangements under these constraints. For example, different permutations of interleaving genes between the syntenic anchors would have equal likelihood of being “ancestral.” In general, the gene groups that have fewer copies may have fewer constraints in the consensus arrangements and therefore cannot be precisely ordered computationally.

## Implications for particular eudicot gene functional groups

By combining available positional information with sequence homologies, our method improves on other orthology/paralogy mapping algorithms that depend mainly on similarity scores, such as OrthoMCL (Li et al. 2003), Inparanoid (O’Brien et al. 2005), and the like. Since the clusters are inferred by syntenic alignments, any gene family constructed by our method contains at least two genes. Genes duplicated by single-gene or tandem duplications do not fall on collinear chains, and thus are excluded from the syntenic gene groups by our algorithm. In contrast, since some of these small-scale duplications are recent and show higher similarities than the paleo-duplicates, they are more easily included by traditional homology-based clustering methods.

The exponential growth in gene numbers resulting from recurring polyploidies is often tempered by a massive yet progressive amount of gene death in the subsequent diploidization process. However, the probability of gene loss is not uniformly distributed among all gene functional groups (Maere et al. 2005). Convergent restoration of some genes to singleton status after multiple rounds of duplication in independent lineages suggests that there may be selective advantages for the organism to have only single copies of these genes (Paterson et al. 2006). However, the most extreme cases of “duplication resistance,” gene functional groups for which one and only one copy per nucleus is adaptive, would provide too little information to be inferred as duplication-resistant by previous  $\chi^2$ -based statistical methods (Paterson et al. 2006). Multi-alignment improves our ability to identify candidate duplication-resistant genes that fall into this most extreme category, in that if a single gene is always restored to singleton following a sufficient number of independent duplications, then duplication resistance of that single gene might be inferred. Such genes have curiously “resisted” multiple duplication cycles in multiple independent lineages, specifically one round of duplication ( $\gamma$ ) in *Carica* and *Vitis*, two ( $p$ ,  $\gamma$ ) in *Populus*, three ( $\alpha$ ,  $\beta$ ,  $\gamma$ ) in *Arabidopsis*, and one ( $p$ ) or more in *Oryza*. Indeed, some syntenic groups have preserved exactly one copy in the ancestral location for each of the five species. Some genes in these groups are not true “singletons,” with non-syntenic copies present in the genome because of single gene duplications. After filtering out such non-syntenic copies, we found 47 strict singleton groups for five angiosperm genomes preserved in collinear linkage groups, supporting their inferred orthology to one another. If we assume that the diploidization process is completely independent in each of the five species, we can estimate the expected number of singleton groups by multiplying the proportions of singleton genes in each genome by the average gene number. Under this estimate, the 47 singleton groups we found are nearly 10 times more than the expected five groups. We also found 247 strict singleton groups for only the four eudicot genomes (versus 20 explicable by chance). The gene IDs and functional annotations for the singleton groups are available in Supplemental Data 5. Many of the singleton genes have only putative classifications, and those of known functions are mostly enzymes.

The multiplicities in ancestral loci constructed by MCscan also revealed extreme cases in which ancestral loci were “deletion-resistant,” with a tendency to be preserved in consistently high copy numbers in multiple species (Table 5). Since both *Carica* and *Vitis* have only one round of duplication with multiplicity of 3, while *Populus* has two rounds of duplications and

**Table 5.** Thirty ancestral loci selected based on saturated paleolog copy numbers in *Carica* ( $\geq 3$  copies), *Populus* ( $\geq 5$  copies), and *Vitis* ( $\geq 3$  copies)

Ancestral locus ID	<i>Carica</i>	<i>Populus</i>	<i>Vitis</i>	<i>Arabidopsis</i>	Gene family <sup>b</sup>
N00011	3	6	3	4	
N00123	3	6	3	3	
N00137	3	6	3	6	
N00535	3	6	3	5	GRAS transcription factor
N00715	3	5	3	3	
N01470	3	6	3	8	
N01482 <sup>a</sup>	3	6	3	7	C2H2 transcription factor
N01483 <sup>a</sup>	3	5	3	10	
N01501	4	5	3	6	
N01504	3	5	3	6	
N01732	3	6	3	8	
N01831	3	5	3	3	
N02420	3	5	3	6	C3H transcription factor
N02938	3	6	3	3	
N03063	3	6	3	6	
N03148	3	5	3	3	Phosphatidylinositol-4-kinase g
N03158	3	5	3	4	
N03159	3	6	3	5	C2C2-Dof transcription factor
N03285	3	5	3	3	Lateral organ boundaries gene, class II
N03326	3	5	3	3	
N03658	3	5	3	4	
N03794	3	5	3	4	
N04406	3	5	3	6	Kinesin-like proteins
N05304	3	6	3	4	C3H transcription factor
N05519	3	6	3	3	EF-hand containing proteins: Group IV
N05829	3	5	3	5	MADS transcription factor
N05866	3	6	4	6	AP2-EREBP transcription factor
N06369	3	5	3	5	C2C2-Gata transcription factor
N07685	3	6	3	3	Lateral organ boundaries gene, class II
N07692	3	6	3	3	Core cell cycle genes

The ancestral loci reference IDs are available in Supplemental Data 3.

<sup>a</sup>Used in the phylogenetic reconstruction in Figure 5.

<sup>b</sup>Based on curated *Arabidopsis* gene families from TAIR (Huala et al. 2001).

multiplicity of 6, we specifically selected the ancestral loci that are saturated with paleologs for these three species, requiring that the groups that we chose have *Carica* multiplicity  $\geq 3$ , *Populus* multiplicity  $\geq 5$ , and *Vitis* multiplicity  $\geq 3$  at the same time (Table 5). We set these copy number cutoffs because *Carica*, *Populus*, and *Vitis* have expected copy numbers of 3, 6, and 3 respectively, and we slightly loosened the *Populus* cutoff to look at more groups that are close to saturation. A total of 30 such groups were found (Table 5). Considering that very few groups have exceeded the threshold for each species (Table 2), the chance that 30 random groups satisfy all three thresholds is almost non-existent ( $\chi^2$ -test,  $P = 2.2 \times 10^{-16}$ ).

In contrast to “duplication-resistant” genes, many “deletion-resistant” loci of known function are transcription factors, consistent with previous findings that transcriptional regulators are significantly over-retained in WGD duplicates (Seoighe and Gehring 2004; Freeling and Thomas 2006). For example, N05829 contains five *Arabidopsis* MADS-box genes (*AGL14*, *AGL19*, *SOC1*, *AGL42*, *AGL72*), all descended from a single ancestral pre- $\gamma$  MADS-box gene. N03285 (contains *Arabidopsis* genes *LBD40*, *LBD41*, *LBD42*) and N07685 (contains *Arabidopsis* genes *LBD37*, *LBD38*, *LBD39*) collectively comprise all six class II lateral organ boundaries (LOB) gene family members characterized to date (Shuai et al. 2002), which we infer to trace to two ancestral (pre- $\gamma$ ) LOB class II genes.

Comparative analysis for genes derived from “deletion-resistant” loci that have largely expanded following each round

of polyploidy have important implications for studying plant gene family evolution. Because of less gene loss, such gene families show improved power to resolve particular evolutionary events. Using two ancestral loci that are close to each other in the local ancestral order and highly saturated with paleo-duplicates, N01482 (C2H2 transcription factor family) and N01483 (auxin-response protein), we constructed phylogenetic trees for the gene members. Both phylogenetic trees (Fig. 5) support the coarse partitioning of three subclades, with each clade containing up to four *Arabidopsis* genes, two *Populus* genes, one *Carica* gene, and one *Vitis* gene. These two examples also support the inference that *Arabidopsis* genes evolve more quickly than *Vitis* genes. This is reflected by the longer branches, that is, more nucleotide substitutions for *Arabidopsis* genes within individual subclades. Indeed, differential evolutionary rates have some impact on the N01482 tree topology, as one *Vitis* gene (*Vv4g1235*) appears to be even closer to one of its  $\gamma$  paleologs (*Vv18g1188*) than to its orthologs in the three other species. One possible alternative explanation is that these two *Vitis* genes have undergone homogenization, as has been shown to occur in some paleo-duplicated genes in *Oryza* genome (Wang et al. 2007).

## Methods

### Gene set and sequence homology search

Protein sequences from *Arabidopsis*, *Carica*, *Populus*, *Vitis*, and *Oryza* genome annotations were used (Table 1). A few annotated moss (*Physcomitrella patens*) genes (JGI annotation version 1.1) were also used as the outgroup in gene tree analysis. *Carica*, *Populus*, and *Vitis* gene names were renamed according to their incremental position on the chromosomes or scaffolds (see Supplemental Data 4 for a conversion table to original gene identifiers). In case the original gene identifiers are subject to future changes, the conversion table will be updated accordingly to ensure easy translation. If a gene had more than one transcript, only the first transcript in the annotation was considered. Each genome was compared against itself and other genomes using BLASTP (Altschul et al. 1990), retrieving the best five hits meeting an *E*-value threshold of  $1 \times 10^{-5}$ .

### Pairwise gene order alignments

The syntenic regions were grouped to form multiple alignments using a novel algorithm MCscan (multiple collinearity scan). We first took whole-genome BLASTP results and computed strictly collinear segments for all possible pairs of chromosomes and scaffolds. A pairwise alignment procedure was implemented using an empirical scoring scheme similar to that of Haas et al. (2004). The default scoring scheme (configurable) is  $\min(\log_{10} E, 50)$  match score for one gene pair, and  $-1$  gap penalty for each 10-kb distance between any two consecutive gene pairs. The

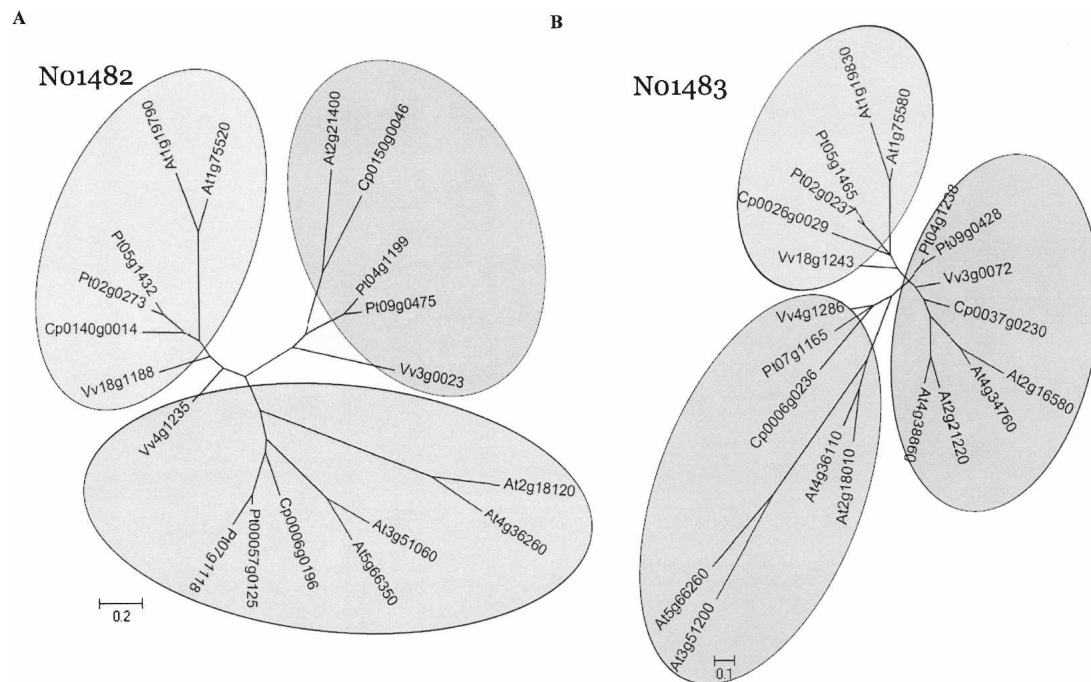


**Figure 5.** Phylogenetic analysis of ancestral loci N01482 (A) and N01483 (B). Coding sequences of all members in four eudicot species for each ancestral locus (19 genes in N01482, 21 in N01483) were aligned by CLUSTALW (Thompson et al. 1994) using parameters suggested by Hall (2007). Phylogenetic relationships among the members and sequences were grouped into clades using MrBayes (Ronquist and Huelsenbeck 2003). The Bayesian analysis was carried out for 500,000 generations using the General Time Reversible plus Gamma (GTR+G) substitution model selected based on MODELTEST (Posada and Crandall 1998). All branches with support <50% are collapsed into a polytomy. A majority tree was presented in both cases. The gene names for *Carica*, *Populus*, and *Vitis* are recoded to reflect relative orders on chromosome or scaffold (see Methods). The conversions from the original locus identifiers to the re-indexed gene names are available as a conversion table in Supplemental Data 4. In case the original gene identifiers are subject to future changes, the conversion table will be updated accordingly. *Arabidopsis* gene names follow their standard TAIR locus IDs. Scale bars represent the number of substitutions per site following the GTR+G model.

score for each pairwise collinear chain is then calculated via dynamic programming through the following recurrence condition, assuming that two gene pairs,  $u$  and  $v$ , are on the path where  $u$  precedes  $v$ ,

$$\text{ChainScore}(v) = \text{MatchScore}(v) + \max_u \{ \text{ChainScore}(u) + \text{GapPenalty}(u,v), 0 \}$$

Tandem matches <50 kb apart are collapsed using a representative pair that has the smallest BLASTP  $E$ -value. This threshold, indeed, did not purge all tandems—we still found a very few long-distance tandems in our clustered ancestral loci—however, this is reasonable trade-off since increasing the threshold would remove some of the intra-chromosomal WGD duplicates. All pairwise segments with scores above 300 are reported. Each pairwise segment consists of two distinct genomic locations with aligned, collinear genes as anchors.

The expected number of occurrences of a pairwise collinearity pattern could be estimated with the following, similar to the one used in Wang et al. (2006),

$$E = 2P_N^m \prod_{i=1}^{m-1} \left( \frac{l_{1i}}{L_1} \cdot \frac{l_{2i}}{L_2} \right),$$

where  $N$  is the number of matching gene pairs (by BLASTP or BLAT, etc.) between two chromosomal regions defined by the syntenic block;  $m$  is the number of collinear gene pairs in the identified block;  $L_1$  and  $L_2$  are respective lengths of the two chromosomal regions; and  $l_{1i}$  and  $l_{2i}$  are distances between two adjacent collinear gene pairs in the syntenic block. The expectation

multiplies by two since there are two possible orientation configurations between two collinear segments. This is only an approximation to a more rigorous yet computationally expensive permutation test (Van de Peer 2004) and Monte Carlo methods (Hampson et al. 2005); however, computational experiments and analytical results (Wang et al. 2006) suggest that this gives a reasonable estimate for the significance of the syntenic blocks. All the pairwise alignments that we reported are significant at  $E < 1 \times 10^{-10}$ .

### Multiple gene order alignments

Pairwise syntenic matches were clustered into multi-way anchors through a Markov clustering algorithm MCL (Enright et al. 2002), in order to simplify the correspondences among multiple loci. Multiple chromosomal regions threaded by consecutive ancestral loci are recovered and aligned using a heuristic that constructs the multiple alignments progressively by aligning one closest-related region at a time by dynamic programming. We then use a reference genome to report all the multiple blocks. Notice that when we use a “reference” as the basis, we lose symmetry. For example, let us assume A-B-C as a multiple alignment, formed by syntenic regions A, B, and C. If we allow the blocks to be threaded by A, B, or C, we can find this block three times; however, the resulting multiple alignment may be slightly different because of the order in which we stack A, B, and C. We found that the “once a gap, always a gap” rule applies to the multiple alignment of gene orders, in that the order of progressive stacking does affect the resulting alignment. Therefore, we implement a refinement procedure to ameliorate such effect by

iteratively realigning each segment, allowing the falsely placed gaps to be corrected and further optimize the gap placement.

### Clustering the multiply-aligned genomic regions

If we consider “gene retention at the ancestral locus” as the ancestral state and “gene loss” as derived, then each aligned chromosomal segment can be described as a vector of binary characters. We could then search for hierarchical clustering based on “Camin-Sokal parsimony” since genes that had been lost are highly unlikely to re-emerge at original paleologous locations, that is, reversal to the ancestral state is prohibited (Camin and Sokal 1965). Using this simplistic parsimony principle, syntenic genomic regions in multiple alignment blocks can be clustered, using the “mix” program in the PHYLIP package (Retief 2000) with 0/1-coded chromosomal regions within each block as input.

### MCscan implementation and availability

The multi-aligned plant gene orders and implemented algorithm and C++ source codes are publicly available (<http://chibba.agtec.uga.edu/duplication/mcscan/>). The program uses only two input files—a file containing BLASTP results and a file describing gene coordinates—and outputs both pairwise syntenic blocks and the multi-aligned gene orders threaded by a reference genome. There are several parameters to configure according to the user’s need. For example, the significance cutoff would reduce sensitivity but increase specificity for the uncovered syntenic blocks.

### Comparison between *Vitis* and *Solanum*, *Musa*

For *Solanum*, we downloaded 195-nt sequences for tomato (*Solanum lycopersicum*) from NCBI (September 2007) that were  $\geq 100$  kb, discarding one chloroplast sequence from analysis, for a total of 25 Mb (representing  $\sim 2.5\%$  of the tomato genome). We retrieved 53,792 TIGR *Solanum* unigenes (*S. lycopersicum* TIGR transcript assembly version 5), mapping them to the collected BACs (BLASTN  $E$ -value  $< 1 \times 10^{-6}$ ) and took the best hit that had  $\geq 200$ -bp alignment length and 97% identity. This should accommodate minor sequencing errors or cultivar differences between the ESTs and BACs, if any. If multiple unigenes went within 300 bp on the tomato sequence, only the longest hit was retained. This was to resolve cases in which the unigenes were not assembled completely or correctly for a gene and the real gene was represented by more than one unigene. A total of 2243 *Solanum* unigenes, 4.2% of the total, were anchored to BACs. *Solanum* unigenes were assigned their base-pair locations within the BACs, and we used these mapped unigenes as tentative gene models on these *Solanum* BACs. The mapped unigenes were then searched for homology against the *Vitis* proteins using BLASTX ( $E < 1 \times 10^{-5}$ ). We analyzed synteny of *Vitis* chromosomal regions and 17 banana (*Musa acuminata*) BACs in a similar procedure.

### Synonymous substitution ( $K_s$ ) and fourfold degenerate site transversion (4DTV) calculation

For each pair of homologs, we aligned their protein sequences using CLUSTALW (Thompson et al. 1994) and converted the protein alignment to DNA alignment using PAL2NAL (Suyama et al. 2006). Some homologous genes could not produce reliable CLUSTALW alignment for various reasons and were discarded from further analysis.  $K_s$  values were calculated using the Nei-Gojobori algorithm (Nei and Gojobori 1986) implemented in the PAML package (Yang 1997). We repeated the  $K_s$  calculation using other algorithms and found that the differences are small, systematic biases that do not affect major conclusions. We calcu-

lated 4DTV values between gene pairs using in-house Perl scripts. 4DTV values are calculated for gene pairs having  $\geq 10$  fourfold degenerate sites. Fourfold degenerate sites are codons of amino acid residues G, A, T, P, V, and R, S, L. Raw 4DTV values are then corrected for possible multiple transversions at the same site using this formula:

$$4DTV_{corrected} = -1/2 \times \ln(1 - 2 \times 4DTV_{uncorrected}).$$

### Finite mixture models of genome duplications based on $K_s$ distribution

The actual distribution of  $K_s$  between paleologs can be modeled as mixtures of log-transformed exponentials and normals, representing single gene duplications and whole genome duplications, respectively. Since we have identified the paralogs that show segmental correspondence with most of the single gene duplications excluded, the actual distributions can be described as mixtures of log-normal components that represent multiple rounds of genome duplications, using the EMMIX software (<http://www.maths.uq.edu.au/~gjm/emmix/emmix.html>).  $K_s$  values that are  $< 0.005$  were discarded to avoid fitting a component to infinity (Cui et al. 2006), and the mixed populations were modeled with one to five components. We selected one best mixture model for each paleolog distribution on the basis of Bayesian information criterion (BIC) and an additional restriction on the mean/variance structure for  $K_s$  (Cui et al. 2006).

### Acknowledgments

We appreciate financial support from the U.S. National Science Foundation (MCB-0450260 to A.H.P. and J.E.B., DBI-0421803 to R.M. and A.H.P.), the University of Hawaii to M.A., and the U.S. Department of Defense W81XWH0520013 to M.A. We thank Guojun Li for helpful discussions on the synteny deduction algorithm.

### References

- Altschul, S.F., Gish, W., Miller, W., Myers, E.W., and Lipman, D.J. 1990. Basic local alignment search tool. *J. Mol. Biol.* **215**: 403–410.
- Arabidopsis* Genome Initiative. 2000. Analysis of the genome sequence of the flowering plant *Arabidopsis thaliana*. *Nature* **408**: 796–815.
- Aury, J.M., Jaillon, O., Duret, L., Noel, B., Jubin, C., Porcel, B.M., Segurens, B., Daubin, V., Anthouard, V., Aiach, N., et al. 2006. Global trends of whole-genome duplications revealed by the ciliate *Paramecium tetraurelia*. *Nature* **444**: 171–178.
- Blanc, G. and Wolfe, K.H. 2004. Widespread paleopolyploidy in model plant species inferred from age distributions of duplicate genes. *Plant Cell* **16**: 1667–1678.
- Blanc, G., Hokamp, K., and Wolfe, K.H. 2003. A recent polyploidy superimposed on older large-scale duplications in the *Arabidopsis* genome. *Genome Res.* **13**: 137–144.
- Blanchette, M., Kent, W.J., Riemer, C., Elnitski, L., Smit, A.F., Roskin, K.M., Baertsch, R., Rosenbloom, K., Clawson, H., Green, E.D., et al. 2004. Aligning multiple genomic sequences with the threaded blockset aligner. *Genome Res.* **14**: 708–715.
- Bowers, J.E., Chapman, B.A., Rong, J., and Paterson, A.H. 2003. Unravelling angiosperm genome evolution by phylogenetic analysis of chromosomal duplication events. *Nature* **422**: 433–438.
- Camin, J.H. and Sokal, R.R. 1965. A method for deducing branching sequences in phylogeny. *Evolution Int. J. Org. Evolution* **19**: 311–326.
- Cui, L., Wall, P.K., Leebens-Mack, J.H., Lindsay, B.G., Soltis, D.E., Doyle, J.J., Soltis, P.S., Carlson, J.E., Arumuganathan, K., Barakat, A., et al. 2006. Widespread genome duplications throughout the history of flowering plants. *Genome Res.* **16**: 738–749.
- Davies, T.J., Barraclough, T.G., Chase, M.W., Soltis, P.S., Soltis, D.E., and Savolainen, V. 2004. Darwin’s abominable mystery: Insights from a supertree of the angiosperms. *Proc. Natl. Acad. Sci.* **101**: 1904–1909.
- Enright, A.J., Van Dongen, S., and Ouzounis, C.A. 2002. An efficient algorithm for large-scale detection of protein families. *Nucleic Acids Res.* **30**: 1575–1584.

- Felsenstein, J. 2004. *Inferring phylogenies*. Sinauer, Sunderland, MA.
- Freeling, M. and Thomas, B.C. 2006. Gene-balanced duplications, like tetraploidy, provide predictable drive to increase morphological complexity. *Genome Res.* **16**: 805–814.
- Gaut, B.S., Morton, B.R., McCaig, B.C., and Clegg, M.T. 1996. Substitution rate comparisons between grasses and palms: Synonymous rate differences at the nuclear gene *Adh* parallel rate differences at the plastid gene *rbcL*. *Proc. Natl. Acad. Sci.* **93**: 10274–10279.
- Haas, B.J., Delcher, A.L., Wortman, J.R., and Salzberg, S.L. 2004. DAGChainer: A tool for mining segmental genome duplications and synteny. *Bioinformatics* **20**: 3643–3646.
- Hall, B.G. 2007. *Phylogenetic trees made easy: A how-to manual*, 3d ed. Sinauer, Sunderland, MA.
- Hampson, S.E., Gaut, B.S., and Baldi, P. 2005. Statistical detection of chromosomal homology using shared-gene density alone. *Bioinformatics* **21**: 1339–1348.
- Hittinger, C.T. and Carroll, S.B. 2007. Gene duplication and the adaptive evolution of a classic genetic switch. *Nature* **449**: 677–681.
- Huala, E., Dickerman, A.W., Garcia-Hernandez, M., Weems, D., Reiser, L., LaFond, F., Hanley, D., Kiphart, D., Zhuang, M., Huang, W., et al. 2001. The *Arabidopsis* Information Resource (TAIR): A comprehensive database and web-based information retrieval, analysis, and visualization system for a model plant. *Nucleic Acids Res.* **29**: 102–105.
- International Rice Genome Sequencing Project. 2005. The map-based sequence of the rice genome. *Nature* **436**: 793–800.
- Itoh, T., Tanaka, T., Barrero, R.A., Yamasaki, C., Fujii, Y., Hilton, P.B., Antonio, B.A., Aono, H., Apweiler, R., Bruskiwich, R., et al. 2007. Curated genome annotation of *Oryza sativa* ssp. *japonica* and comparative genome analysis with *Arabidopsis thaliana*. *Genome Res.* **17**: 175–183.
- Jaillon, O., Aury, J.M., Brunet, F., Petit, J.L., Stange-Thomann, N., Mauceli, E., Bouneau, L., Fischer, C., Ozouf-Costaz, C., Bernot, A., et al. 2004. Genome duplication in the teleost fish *Tetraodon nigroviridis* reveals the early vertebrate proto-karyotype. *Nature* **431**: 946–957.
- Jaillon, O., Aury, J.M., Noel, B., Policriti, A., Clepet, C., Casagrande, A., Choisine, N., Aubourg, S., Vitulo, N., Jubin, C., et al. 2007. The grapevine genome sequence suggests ancestral hexaploidization in major angiosperm phyla. *Nature* **449**: 463–467.
- Kellis, M., Birren, B.W., and Lander, E.S. 2004. Proof and evolutionary analysis of ancient genome duplication in the yeast *Saccharomyces cerevisiae*. *Nature* **428**: 617–624.
- Koch, M.A., Haubold, B., and Mitchell-Olds, T. 2000. Comparative evolutionary analysis of chalcone synthase and alcohol dehydrogenase loci in *Arabidopsis*, *Arabis*, and related genera (Brassicaceae). *Mol. Biol. Evol.* **17**: 1483–1498.
- Ku, H.M., Vision, T., Liu, J., and Tanksley, S.D. 2000. Comparing sequenced segments of the tomato and *Arabidopsis* genomes: Large-scale duplication followed by selective gene loss creates a network of synteny. *Proc. Natl. Acad. Sci.* **97**: 9121–9126.
- Kuittinen, H., de Haan, A.A., Vogl, C., Oikarinen, S., Leppala, J., Koch, M., Mitchell-Olds, T., Langley, C.H., and Savolainen, O. 2004. Comparing the linkage maps of the close relatives *Arabidopsis lyrata* and *A. thaliana*. *Genetics* **168**: 1575–1584.
- Li, L., Stoeckert Jr., C.J., and Roos, D.S. 2003. OrthoMCL: Identification of ortholog groups for eukaryotic genomes. *Genome Res.* **13**: 2178–2189.
- Maere, S., De Bodd, S., Raes, J., Casneuf, T., Van Montagu, M., Kuiper, M., and Van de Peer, Y. 2005. Modeling gene and genome duplications in eukaryotes. *Proc. Natl. Acad. Sci.* **102**: 5454–5459.
- Miller, W., Rosenbloom, K., Hardison, R.C., Hou, M., Taylor, J., Raney, B., Burhans, R., King, D.C., Baertsch, R., Blankenberg, D., et al. 2007. 28-Way vertebrate alignment and conservation track in the UCSC Genome Browser. *Genome Res.* **17**: 1797–1808.
- Ming, R., Hou, S., Feng, Y., Yu, Q., Dionne-Laporte, A., Saw, J.H., Senin, P., Wang, W., Ly, B.V., Lewis, K.L., et al. 2008. The draft genome of the transgenic tropical fruit tree papaya (*Carica papaya* Linnaeus). *Nature* **452**: 991–996.
- Nei, M. and Gojobori, T. 1986. Simple methods for estimating the numbers of synonymous and nonsynonymous nucleotide substitutions. *Mol. Biol. Evol.* **3**: 418–426.
- O'Brien, K.P., Remm, M., and Sonnhammer, E.L. 2005. Inparanoid: A comprehensive database of eukaryotic orthologs. *Nucleic Acids Res.* **33**: D476–D480.
- Paterson, A.H., Chapman, B.A., Kissinger, J.C., Bowers, J.E., Feltus, F.A., and Estill, J.C. 2006. Many gene and domain families have convergent fates following independent whole-genome duplication events in *Arabidopsis*, *Oryza*, *Saccharomyces* and *Tetraodon*. *Trends Genet.* **22**: 597–602.
- Posada, D. and Crandall, K.A. 1998. MODELTEST: Testing the model of DNA substitution. *Bioinformatics* **14**: 817–818.
- Retief, J.D. 2000. Phylogenetic analysis using PHYLIP. *Methods Mol. Biol.* **132**: 243–258.
- Ronquist, F. and Huelsenbeck, J.P. 2003. MrBayes 3: Bayesian phylogenetic inference under mixed models. *Bioinformatics* **19**: 1572–1574.
- Scannell, D.R., Frank, A.C., Conant, G.C., Byrne, K.P., Woolfit, M., and Wolfe, K.H. 2007. Independent sorting-out of thousands of duplicated gene pairs in two yeast species descended from a whole-genome duplication. *Proc. Natl. Acad. Sci.* **104**: 8397–8402.
- Seoighe, C. and Gehring, C. 2004. Genome duplication led to highly selective expansion of the *Arabidopsis thaliana* proteome. *Trends Genet.* **20**: 461–464.
- Shuai, B., Reynaga-Pena, C.G., and Springer, P.S. 2002. The lateral organ boundaries gene defines a novel, plant-specific gene family. *Plant Physiol.* **129**: 747–761.
- Soltis, D.E., Soltis, P.S., Endress, P.K., and Chase, M.W. 2005. *Phylogeny and evolution of angiosperms*. Sinauer Associates, Sunderland, MA.
- Spillane, C., Schmid, K.J., Laouelle-Duprat, S., Pien, S., Escobar-Restrepo, J.M., Baroux, C., Gagliardini, V., Page, D.R., Wolfe, K.H., and Grossniklaus, U. 2007. Positive Darwinian selection at the imprinted MEDEA locus in plants. *Nature* **448**: 349–352.
- Sterck, L., Rombauts, S., Vandepoele, K., Rouze, P., and Van de Peer, Y. 2007. How many genes are there in plants (... and why are they there)? *Curr. Opin. Plant Biol.* **10**: 199–203.
- Suyama, M., Torrents, D., and Bork, P. 2006. PAL2NAL: Robust conversion of protein sequence alignments into the corresponding codon alignments. *Nucleic Acids Res.* **34**: W609–W612.
- Tang, H., Bowers, J., Wang, X., Ming, R., Alam, M., and Paterson, A. 2008. Synteny and collinearity in plant genomes. *Science* **320**: 486–488.
- Thomas, B.C., Pedersen, B., and Freeling, M. 2006. Following tetraploidy in an *Arabidopsis* ancestor, genes were removed preferentially from one homeolog leaving clusters enriched in dose-sensitive genes. *Genome Res.* **16**: 934–946.
- Thompson, J.D., Higgins, D.G., and Gibson, T.J. 1994. CLUSTAL W: Improving the sensitivity of progressive multiple sequence alignment through sequence weighting, position-specific gap penalties and weight matrix choice. *Nucleic Acids Res.* **22**: 4673–4680.
- Tuskan, G.A., Difazio, S., Jansson, S., Bohlmann, J., Grigoriev, I., Hellsten, U., Putnam, N., Ralph, S., Rombauts, S., Salamov, A., et al. 2006. The genome of black cottonwood, *Populus trichocarpa* (Torr. & Gray). *Science* **313**: 1596–1604.
- Van de Peer, Y. 2004. Computational approaches to unveiling ancient genome duplications. *Nat. Rev. Genet.* **5**: 752–763.
- Vandepoele, K., Saey, Y., Simillion, C., Raes, J., and Van De Peer, Y. 2002. The automatic detection of homologous regions (ADHoRe) and its application to microcolinearity between *Arabidopsis* and rice. *Genome Res.* **12**: 1792–1801.
- Wang, X., Shi, X., Li, Z., Zhu, Q., Kong, L., Tang, W., Ge, S., and Luo, J. 2006. Statistical inference of chromosomal homology based on gene colinearity and applications to *Arabidopsis* and rice. *BMC Bioinformatics* **7**: 447. doi: 10.1186/1471-2105-7-447.
- Wang, X., Tang, H., Bowers, J.E., Feltus, F.A., and Paterson, A.H. 2007. Extensive concerted evolution of rice paralogs and the road to regaining independence. *Genetics* **177**: 1753–1763.
- Yang, Z. 1997. PAML: A program package for phylogenetic analysis by maximum likelihood. *Comput. Appl. Biosci.* **13**: 555–556.
- Zhang, Y., Xu, G.H., Guo, X.Y., and Fan, L.J. 2005. Two ancient rounds of polyploidy in rice genome. *J. Zhejiang Univ. Sci. B* **6**: 87–90.

Received May 15, 2008; accepted in revised form September 2, 2008.